

ANALYSIS AND MODELING OF PRESSURE INDUCED BY SEPARATED REATTACHING FLOWS

W.W. H. Yeung

School of Mechanical and Production Engineering, Nanyang Technological University

Keywords: vortex, separation, reattachment, pressure

Abstract

Recent experimental measurements indicate that a backward-facing step located on the suction side of an NACA23012 airfoil may produce greater lift and lift-to-drag-ratio over a broader range of operational angles of attack. Flow-visualization studies confirm the presence of a standing vortex created by the separated reattaching flow. This paper presents an analysis on the mean pressure data induced by such type of flow downstream of a variety of two-dimensional bodies to reveal some similarity features that have been overlooked previously. For instance, the step height has been identified as an important parameter in the correlation between the reattachment length and the initial shear-layer angle. The separation velocity in the direction perpendicular to the upstream flow increases linearly with the reattachment length at fixed step heights. The streamwise location of the vortex center correlates with the location of minimum pressure, each varying linearly with the reattachment length. Lift, moment and center of pressure also increase with the reattachment length. An inviscid flow model of a stationary vortex above a flat wall is proposed and the induced pressure in reduced coordinates are comparable with experimental measurements.

1 Introduction

The increasing demand for additional lift and high wing loads for vertical and short takeoff and landing aircraft leads to continual research on lift enhancement. Earlier powered high-lift systems include slotted and externally blown

flaps, the boundary-layer control, and the augmentor-wing concept.

Recently, the experimental measurements in [1] indicate that a backward-facing step located on the “suction” side of an NACA23012 airfoil may produce greater lift and lift-to-drag-ratio over a broader range of operational angles of attack at a chord-Reynolds number of 4.7×10^5 . With a step height equal to 50% of the local thickness of an NACA 23012 profile, a substantial enhancement in lift was found for a wide range of α , as shown in Fig. 1a. The corresponding improvement in lift-to-drag ratio (especially in the post-stall zone) at the same Reynolds number is depicted in Fig. 1b.

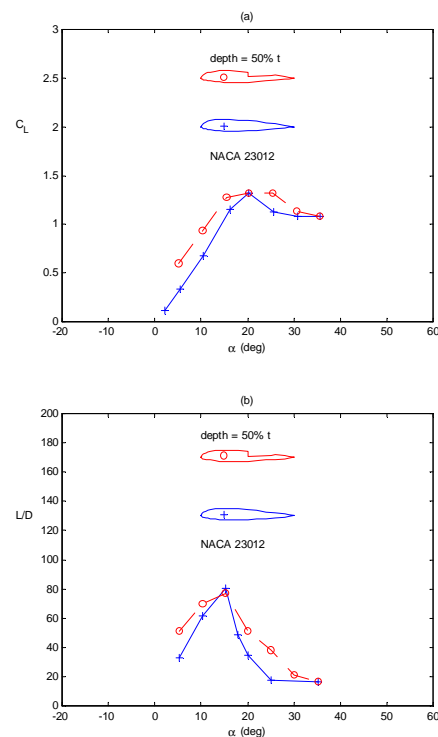


Fig. 1 The variations of (a) lift C_L and (b) lift-to-drag ratio L/D with angle of attack α of NACA 23012 airfoil with and without a step from [1].

The flow-visualization pictures in [2] depict that the flow over the airfoil surface separates at the edge of the backward-facing step and reattaches onto to the remaining portion of the airfoil to form a re-circulation zone dominated by a clockwise-rotating vortex. Their computational results using the commercially available code CFDS-Flow3D reveal that a similar step on the “pressure” side may also lead to considerable enhancements in performance.

To further understand the nature of such flow, an analysis is carried out here on the mean pressure data induced by separated reattaching flow downstream of a variety of two-dimensional bodies to reveal some similarity features that have been overlooked previously. The step height has been identified as an important parameter in the correlation between the reattachment length and the initial shear-layer angle. The velocity at separation in the direction perpendicular to the upstream flow is found to increase linearly with the reattachment length at fixed step heights. The stream-wise location of the vortex center correlates with the location of minimum pressure, each varying linearly with the reattachment length. Lift, moment and center of pressure also increase with the reattachment length. An inviscid flow model of a stationary rotational vortex above a flat wall is proposed, leading to a general form of the pressure recovery comparable with experimental measurements. It also demonstrates that the present analyses and the theoretical model enable the pressure distributions to be realistically predicted.

2 Step Height and Shear-layer Angle

Based on the experimental data of [3] and others, [4] proposed a relationship between the reattachment length x_r/H and the angle of flow separation (or initial shear-layer angle) θ for separated reattaching flows involving a wide range of fore-body geometry, namely

$$\frac{x_r(\theta) - x_r(0^\circ)}{x_r(90^\circ) - x_r(0^\circ)} = \sin \theta \quad (1)$$

where H is the maximum body thickness. Fig. 2 is a sketch of the mean flow pattern behind a wedge of apex angle 2θ , showing the extent of the separated reattaching flow within the range $0 < x \leq x_r$ and the corresponding pressure distribution. Some of the geometrical and physical parameters identified in the present study such as θ and x_r are also defined in Fig. 2. It is noted that $c_p = 2(p - p_\infty)/(\rho U^2)$, which is the usual pressure coefficient. $\theta = 0^\circ$ and 90° correspond to the backward-facing step and the vertical fence with a splitter plate downstream, respectively.

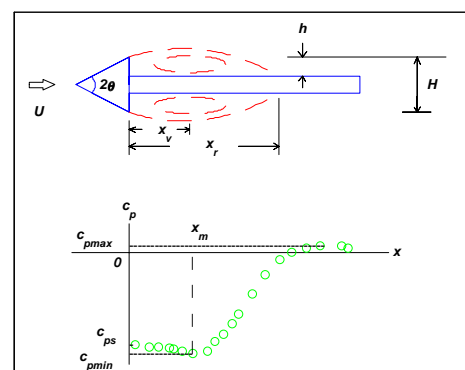


Fig. 2 The definition sketch of pertinent parameters used in the present study.

Fig. 3 shows that eqn. (1) is a good fit to most of data from [3], where the step height h , defined as the vertical distance between separation and reattachment, is about $0.37H$.

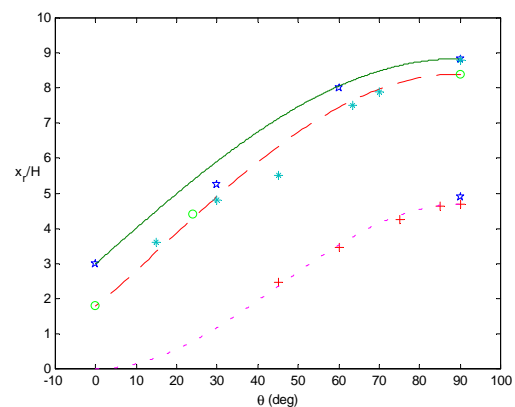


Fig. 3 The variation of reattachment length x_r/H with initial shear-layer angle θ . ☆: from [3], +: from [5], ○: from [6], *: from [7], —: eqn (1), - - -: eqn. (2), - · - · -: eqn (3).

The exceptional data point is associated with the blunt-plate model ($\theta = 90^\circ$, $h/H = 0$), and is seen to lie much lower than the point with $\theta = 90^\circ$ and $h/H = 0.37$. It, however, follows the trend of data from [5], where it was studied how θ would affect the separated reattaching flow (or “separation bubble”) above a blunt plate of thickness H (i.e. $h/H = 0$) fitted with a frontal piece to allow θ to be 45° , 60° , 75° , 85° or 90° .

A comparison of data [5] and the proposed relationship for $h/H = 0$

$$\frac{x_r(\theta)}{x_r(90^\circ)} = \sin^2 \theta \quad (2)$$

is also given in Fig. 3. If the difference between eqn. (1) and eqn. (2) lies mainly on the step height, then they can be unified as

$$\frac{x_r(\theta, h/H) - x_r(0^\circ, h/H)}{x_r(90^\circ, h/H) - x_r(0^\circ, h/H)} = \sin^n \theta \quad (3)$$

where $x_r(0^\circ, 0) = 0$ and $n = 2 - (h/H)/0.37$. The validity of eqn. (3) is substantiated by comparing it with the data from [6] (where $h/H \approx 0.34$) and [7] (where $h/H \approx 0.32$) in Fig. 3.

In analyzing some of the experimental data on separated flow but without downstream reattachment behind a flat plate at inclination α , [8] found that the separation velocity $u(\alpha) = \sqrt{1 - c_{ps}(\alpha)} \sin \alpha$, where c_{ps} is the pressure coefficient at separation, may be used to define a “characteristic wake width” leading to a modified Strouhal number independent of α . A subsequent study by the same authors found a similar result for separated flow behind a symmetric wedge of arbitrary apex angle.

From Fig. 4, it is interesting to note that the data from [3] and [5] for separated “reattaching” flows, when expressed in terms of the separation velocity $u(\theta) = \sqrt{1 - c_{ps}(\theta)} \sin \theta$ are linearly related to the corresponding characteristic length x_r as

$$u(\theta) = A(x_r/H) + B \quad (4)$$

where A and B are functions of h/H . This suggests an important similarity existing between separated flow and separated “reattaching” flow near separation.

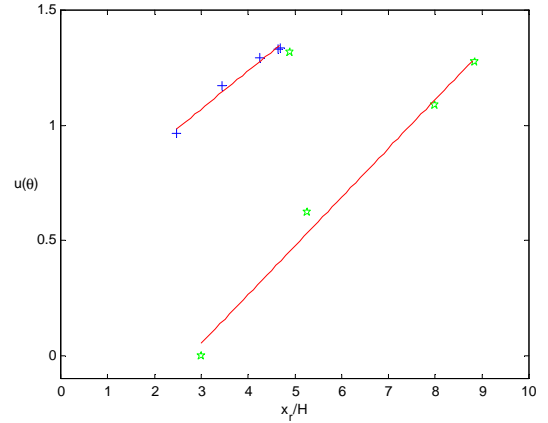


Fig. 4 The variation of dimensionless separation velocity $u(\theta)$ with reattachment length x_r/H . ☆: from [3], +: from [5], —: best linear fit.

3 Location of Standing Vortex

Streamline plots from [9-14] indicate the presence of a standing vortex situated between separation and reattachment. It is well known that a stationary vortex generally induces a low pressure such as that found on an inclined delta wing.

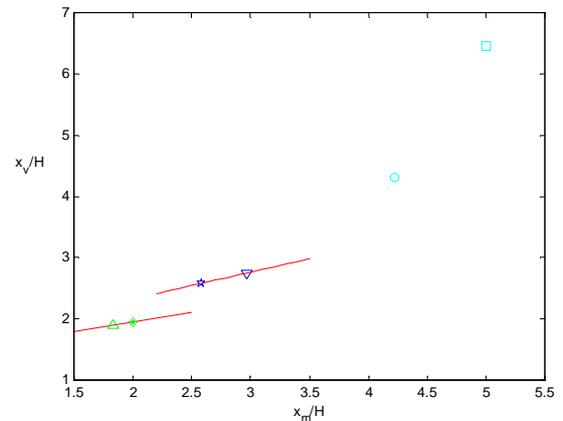


Fig. 5 The location of vortex center x_v/H vs. reattachment length x_r/H . ○: from [9], ●: from [10], ▽: from [11], ■: from [12], ☆: from [13], ☆: from [14], —: best linear fit.

Fig. 5 correlates the location of the standing vortex x_v/H with the location of minimum pressure x_m/H downstream of separation of three different configurations, namely the blunt plate ($h/H = 0$, [10, 14]), the backward-facing step ($0 < h/H < 1$, [11, 13]), the vertical fence with a downstream splitter plate ($h/H = 1$, [9, 10]). The influence of step height is certainly obvious.

Bearing this in mind, data of x_m/H and x_r/H from [3], [5], [6] and [7] are plotted in Figs. 6, 7, 8 and 9 to reveal a linear relationship

$$x_m/H = C + D(x_r/H) \quad (5)$$

where C and D are functions of h/H .

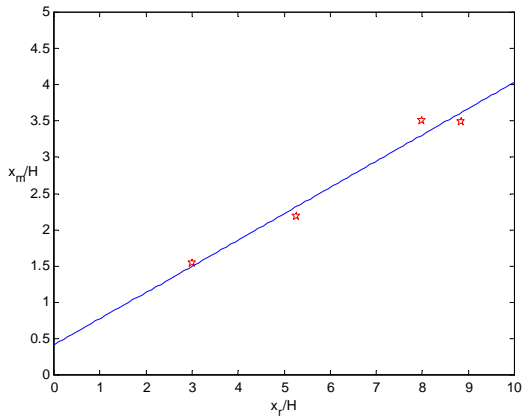


Fig. 6 The location of minimum pressure x_m/H vs. x_r/H from [3]. — : best linear fit (see eqn. (5)).

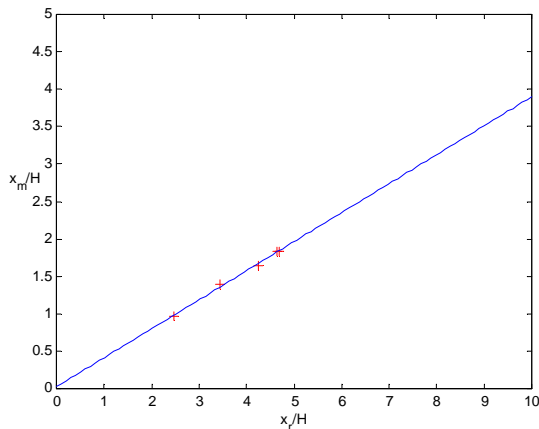


Fig. 7 The location of minimum pressure x_m/H vs. x_r/H from [5]. — : best linear fit (see eqn. (5)).

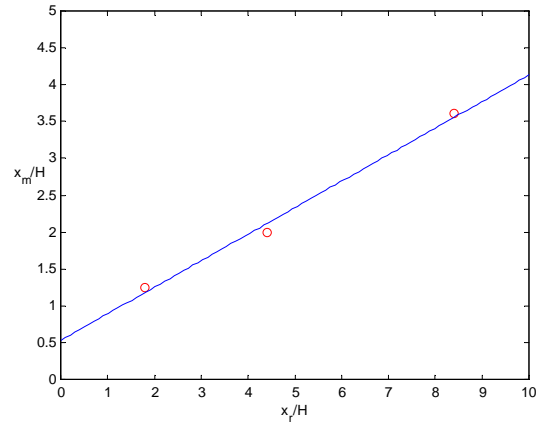


Fig. 8 The location of minimum pressure x_m/H vs. x_r/H from [6]. — : best linear fit (see eqn. (5)).

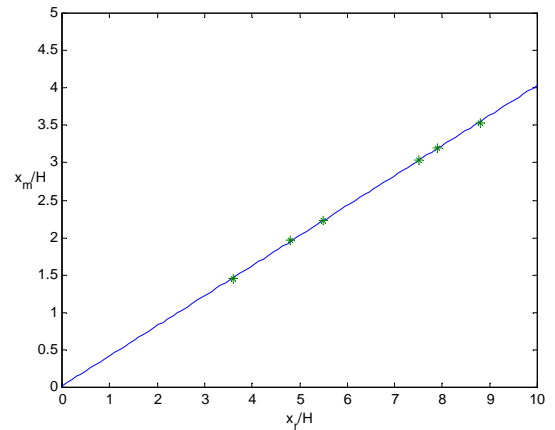


Fig. 9 The location of minimum pressure x_m/H vs. x_r/H from [7]. — : best linear fit (see eqn. (5)).

4 Lift, Moment, Center of Pressure and Pressure Gradient

Let the coefficient of lift, the coefficient of moment and the center of pressure induced by the separated reattaching flow be defined respectively as

$$C_L = \int_{x=0}^{x=x_r} (-c_p) d\left(\frac{x}{H}\right) \quad (6)$$

$$C_M = \int_{x=0}^{x=x_r} \left(\frac{x}{H}\right) (-c_p) d\left(\frac{x}{H}\right) \quad (7)$$

$$z = \frac{C_M}{C_L} \quad (8)$$

where c_p is the usual pressure coefficient and $x = 0$ is the point of separation.

The data from [3] (see Figs. 10, 11 and 12) as well as data from [5], [6] and [7] (not presented here) can be correlated with x_r / H as

$$C_L = E + F(x_r / H) \quad (9)$$

$$C_M = G + I(x_r / H) + K(x_r / H)^2 \quad (10)$$

$$z = M + N(x_r / H) \quad (11)$$

where E, F, G, I, K, M and N are functions of h / H . The linear and quadratic variations in (9), (10) and (11) are surprisingly “simple”, given the non-linear variation of pressure within the separation bubble.

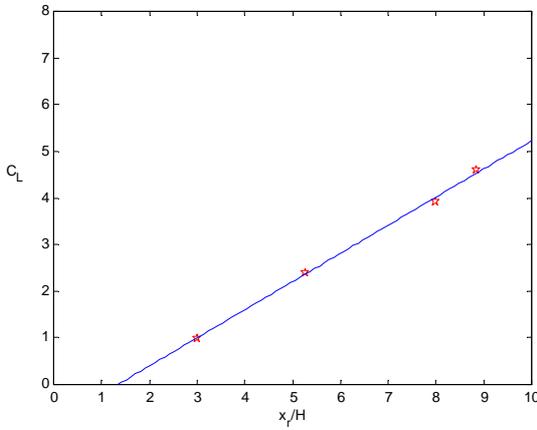


Fig. 10 The variation of lift coefficient C_L with attachment length x_r/H from [3], — : best fit (see eqn. (9)).

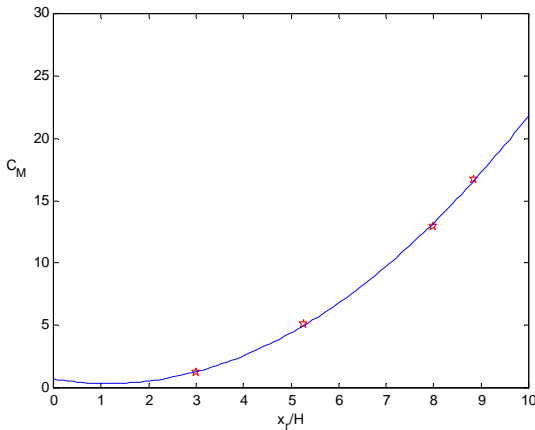


Fig. 11 The variation of moment coefficient C_M with reattachment length x_r/H from [3], — : best fit (see eqn. (10)).

Incidentally, Fig. 10 indicates that the lift induced by the vortex increases with x_r / H . As Fig. 3 shows x_r / H increasing with θ , it is deduced that C_L increases with the separation

angle θ . As such, if the separation angle of the geometry used in [1] (i.e. $\theta = 0^\circ$ for the backward-facing step) is increased, more enhancement in lift is expected.

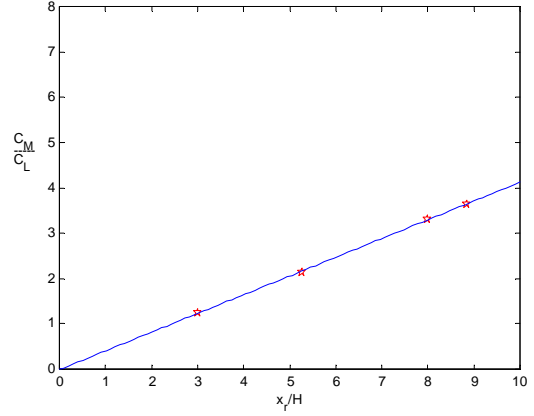


Fig. 12 The variation of center of pressure z with reattachment length x_r/H . ☆ : from [3], — : best fit (see eqn. (11)).

The pressure gradient on a smooth surface has long been considered as an important parameter at the incipient separation such as the case of flow around a circular cylinder. Its importance at reattachment has yet been widely recognized. Here, the pressure gradient $dc_p/d(x/H)$ at reattachment (i.e. $x = x_r$) as shown in Fig. 13 is found to behave like

$$\frac{dc_p}{d(x_r / H)} = \frac{P}{(x_r / H)^Q} \quad (12)$$

where P and Q are functions of h / H .

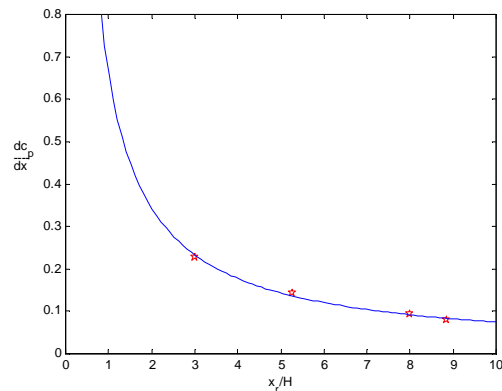


Fig. 13 The variations of pressure gradient $dC_p/d(x_r/H)$ with reattachment length x_r/H from [3], — : best fit (see eqn. 12).

5 Reduced coordinates

Some similarity features of separated reattaching flow were earlier examined in [6]. The hypothesis that the reattachment rise depends on the velocity U_s and pressure p_s approaching separation leads to a new pressure coefficient

$$c_p^* = \frac{p - p_s}{\frac{1}{2} \rho U_s^2} \quad (13)$$

which is related to the usual c_p by

$$c_p^* = \frac{c_p - c_{ps}}{1 - c_{ps}} \quad (14)$$

Note that $c_{ps} = c_p$ at $p = p_s$. As reported in [6], experimental measurements of pressure with thin boundary-layer at separation were found to be collapsed onto a single curve when plotted in terms of c_p^* and $x^* = x/x_r$. Data from [3] of various fore-body shapes as shown in Fig. 14 are plotted in terms of c_p^* and x/x_r in Fig. 15, demonstrating the claim from [6]. As model E has the largest boundary-layer thickness at separation, its c_p^* distribution deviates from those of other models.

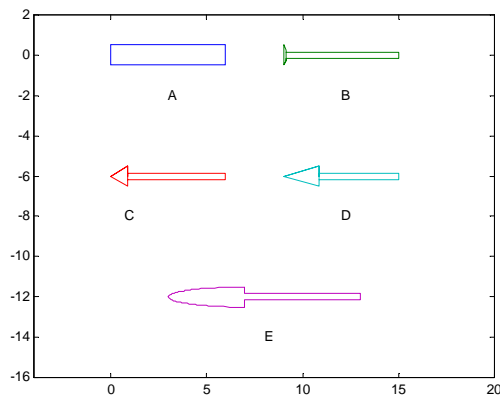


Fig. 14 Models having various fore-body shapes from [3].

Improvements are, however, found when using reduced coordinates

$$c_p^{**} = \frac{c_p - \min(c_p)}{\max(c_p) - \min(c_p)} \quad (15)$$

and

$$x^{**} = \frac{x - x_m}{x_r} \quad (16)$$

as shown in Fig. 16, especially for the pressure distribution of model E. Note that $\max(c_p)$ and $\min(c_p)$ are respectively maximum and minimum values of c_p .

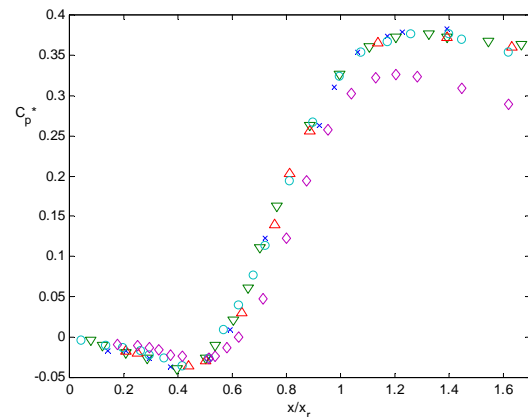


Fig. 15 Comparison of pressure distributions from [3] in reduced coordinates x/x_r and c_p^* . \times , \circ , \square , ∇ , \diamond : models A to E.

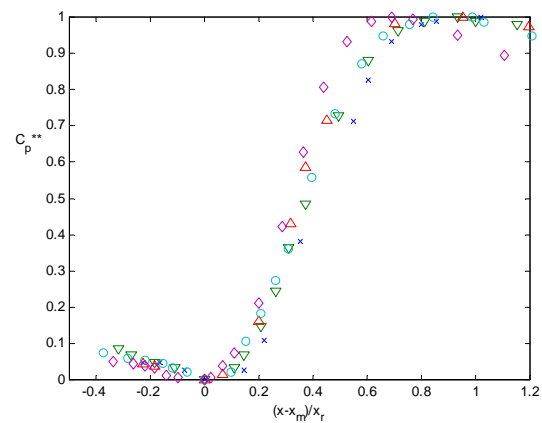


Fig. 16 Comparison of pressure distributions from [3] in reduced coordinates $(x - x_m)/x_r$ and c_p^{**} . \times , \circ , \square , ∇ , \diamond : models A to E.

In Fig. 16 over the range $-0.5 < x^{**} < 0$ (or $0 < x < x_m$), c_p^{**} varies gradually from its value at separation to its minimum value and is accurately represented by

$$c_p^{**} = \frac{\min(c_p) - c_{ps}}{\max(c_p) - \min(c_p)} \frac{x_r}{x_m} x^{**} \quad (17)$$

In fact, it is very often to have $\min(c_p) \approx c_{ps}$.

Over another range $0 < x^{**} < 1 - (x_m/x_r)$ (or $x_m < x < x_r$), the pressure recovers rapidly and non-linearly. The above-mentioned streamline plots from [9-14] suggest that the flow may be modeled with a two-dimensional vortex located at a distance $y=L$ above an impermeable boundary along $y=0$. If the vortex is assumed inviscid and has its vorticity proportional to the stream function, then the stream function ψ satisfies

$$\frac{\partial^2 \psi}{\partial x^2} + \frac{\partial^2 \psi}{\partial y^2} = -k^2 \psi \quad (18)$$

and k^2 is the constant of proportionality (see [15]). It can be shown that the analytical solution in polar coordinates (r, θ) is given by

$$\psi(r, \theta) = 2U \frac{J_1(kr) \sin \theta}{kJ_0(kp)} \quad (19)$$

where J_0 and J_1 are Bessel functions of order zero and one, $kp = 3.83$ (the 1st zero of J_1) and $p = 2.1L$. Fig. 17 depicts some of the streamlines derived from this stream function.

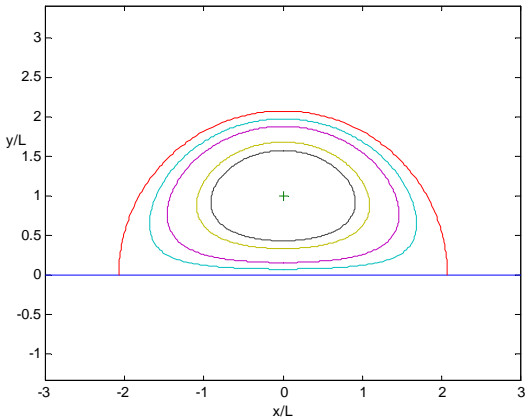


Fig. 17 Streamlines of the flow model.

If $L = 1$ is chosen, then

$$c_p^{**} = 1 - \frac{4J_1^2(kpx^{**})}{(kpx^{**})^2} \quad (20)$$

which is reasonably closed to the data from [3] in $0 < x^{**} < 1 - (x_m/x_r)$, as shown in Fig. 18.

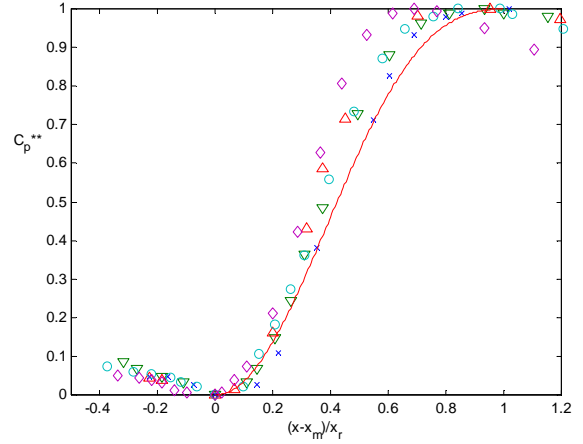


Fig. 18 Comparison of theoretical and experimental pressure distributions in reduced coordinates $(x - x_m)/x_r$ and c_p^{**} . \times , O , ∇ , \diamond : data from [3], —: eqn. 20.

6 Results

Fig. 18 as well as the definitions of c_p^{**} and x^{**} suggests that the pressure distributions be characterized by five parameters, namely $\max(c_p)$, $\min(c_p)$, c_{ps} , x_m/H and x_r/H . They can be solved for from the equations of $u(\theta)$, x_m/H , C_L , z and $dc_p/d(x_r/H)$ as functions of x_r/H together with eqns. (15, 17, 20). Typical plots the theoretical pressure distribution is given in Figs. 19 and 20, in comparison with the experimental measurements from [5] at $\theta = 60^\circ$ and 75° . In general, the prediction is realistic within the region between separation and reattachment.

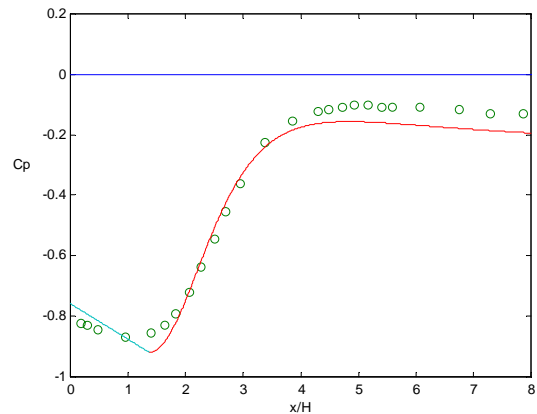


Fig. 19 Comparison of predicted pressure with experimental data ($\theta = 60^\circ$) from [5].

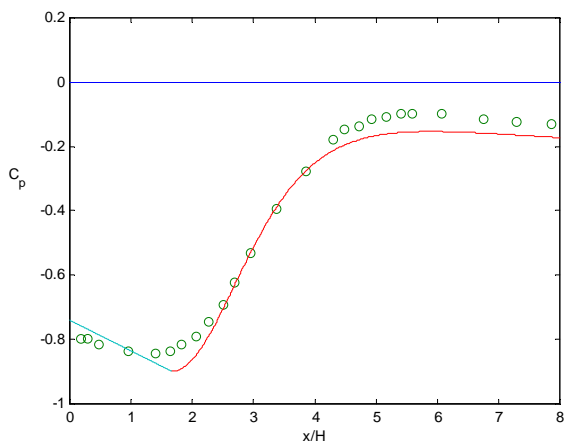


Fig. 20 Comparison of predicted pressure with experimental data ($\theta = 75^\circ$) from [5].

7 Conclusion

Motivated by the experimental measurements and the flow visualization results of induced lift created by a backward-facing step, this paper examines the mean pressure distributions of separated reattaching flows. From the existent data, it is shown that the step height is an important parameter in correlating reattachment length with the initial shear-layer angle. The separation velocity (deduced from the separation pressure) is found to increase linearly with the reattachment length. Other physical quantities such as lift and moment are also correlated with the reattachment length. It is noted that the lift induced by the backward-facing step can be enhanced when the separation angle is enlarged. Using these relationships and a proposed theoretical model, it is shown that the pressure distribution can be reproduced with reasonable accuracy. It is the author's intention to study the unsteadiness of the pressure distributions and examine how they respond to free-stream turbulence in the next phase.

References

- [1] Fertis D. New airfoil-design concept with improved aerodynamic characteristics. *J. Aero. Engng.*, ASCE, Vol. 7, pp 328-339, 1994.
- [2] Finaish F and Witherspoon S. Aerodynamic performance of an airfoil with step-induced vortex for lift augmentation. *J. Aero. Engng.*, ASCE, Vol. 11, pp 9-16, 1998.
- [3] Cherry N, Hillier R and Latour M. The unsteady structure of two-dimensional separated-and-reattaching flows. *J. Wind Eng. Ind. Aero.*, Vol. 11, pp 95-105, 1983.
- [4] Simpson R. Two-dimensional turbulent separated flow. *AGARDograph* 287, 1985.
- [5] Djilali N and Gartshore I. Effect of leading-edge geometry on a turbulent separation bubble. *AIAA J.*, Vol. 30, pp 559-561, 1991a.
- [6] Roshko A and Lau J. Some observations on transition and reattachment of a free shear layer in incompressible flow. *Proc. 1965 Heat transfer and fluid mechanics institute. Stanford University Pres.*, 1965.
- [7] Govinda Ram H and Arakeri V. Studies on unsteady pressure fields in the region of separating and reattaching flows. *ASME: J. Fluids Eng.*, Vol. 112, pp 402-408.
- [8] Yeung W and Parkinson G. On the steady separated flow around an inclined flat plate. *J. Fluid Mech.*, Vol. 333, pp 403-413, 1997.
- [9] Castro I. and Haque A. The structure of a turbulent shear layer bounding a separation region. *J. Fluid Mech.*, Vol. 179, pp 439, 1987.
- [10] Djilali N and Gartshore I. Turbulent flow around a bluff rectangular plate. Part I: Experimental investigation. *ASME: J. Fluids Eng.*, Vol. 110, pp 275, 1991b.
- [11] Driver D, Seegmiller H and Marvin J. Time-dependent behavior of a reattaching shear layer. *AIAA J.*, Vol. 25, pp 914, 1987.
- [12] Good M and Joubert P. The form drag of two-dimensional bluff-plates immersed in turbulent boundary layers. *J. Fluid Mech.*, Vol. 31, pp 547-582, 1968.
- [13] Moss W and Baker S. Re-circulating flows associated with two-dimensional steps. *Aero. Q.*, Vol. 31, pp 151-172, 1980.
- [14] Ota T and Itasaka M. A separated and reattached flow on a blunt flat plate. *ASME: J. Fluids Eng.*, Vol. 98, pp 79-86, 1976.
- [15] Lamb H. *Hydrodynamics*. Dover, 6th edition, 1932.